Pure Appl. Chem., Vol. 72, No. 1, pp. 221–228, 2000.

A complementary study of surface-enhanced Raman scattering and metal nanorod arrays*

J. L. Yao[1], G. P. Pan[2], K. H. Xue[2†], D. Y. Wu[1], B. Ren[1], D. M. Sun[2], J. Tang[1], X. Xu[1] and Z. Q. Tian[1†]

[1]State Key Laboratory for Physical Chemistry of Solid Surfaces and Institute of Physical Chemistry, Xiamen University, Xiamen 361005, China; [2]Department of Chemistry, Nanjing Normal University, Nanjing 210097, China

Abstract: The two-dimensional arrays of various metal nanowires with diameters ranging from 15 to 70 nm have been fabricated by electrodepositing metals of Cu, Ag, Au, Ni, and Co into the nanoholes of the anodic aluminum oxide (AAO) films, followed by partial removal of the film. The strong surface-enhanced Raman scattering (SERS) effects were observed from the metal nanowire arrays including Ni, Co metals that were normally considered to be non-SERS active substrates. It has been shown that metal nanowire arrays can serve as very good SERS active substrates, especially for transition metals. The SERS intensity of the probe molecule adsorbed at the nanowires depends critically on the length of the nanowires explored at the surface. And the band frequency is very sensitive to the diameter, which reflects the change in the electronic property of metal nanowires. Applying this probe molecule strategy, SERS could develop into a diagnostic tool of metal nanowires (nanorods).

INTRODUCTION

The study on nanowires has received tremendous interest recently because of their novel properties and potential applications in wide fields [1–5]. All the sophisticated application of nano-materials must be based on a solid understanding of their novel properties. Many techniques have been employed to deal with this problem, and UV–vis absorption spectroscopy is the most widely used method for characterizing the optical properties and electronic structure of the nanoparticles [2,6–8], as the absorption bands are related to the diameter and aspect ratio of metal and semiconductor nanowires. It can detect the surface plasmon (SP) resonance on the noble metals such as Ag, Au, and Cu, and the width of SP absorption is related to the size of metal nanoparticles. By contrast, Raman spectroscopy has been used in the study of only semiconductor and carbon materials that exhibit certain optical phonon modes [9-12]. Moskovits et al. measured the bandgap energy of the semiconductor nanowires with different wire diameters by using resonance Raman spectroscopy with different excitation wavelength [9]. A key feature of the nano-scale carbon and semiconductors is that some forbidden Raman modes in bulk materials become Raman active so as to provide important information through Raman studies [11,12]. Unfortunately, nano-scale metals themselves can only exhibit the mechanical vibration bands (also called inelastic Mie scattering or acoustic modes) located in extremely low frequency region (typically 2–10 cm^{-1}) [13]. Therefore, we take an alternative approach to the use of Raman spectroscopy to study metal nanowires by applying probe molecule strategy.

Surface-enhanced Raman spectroscopy (SERS) with extremely high sensitivity can easily detect slightly spectral change of surface species, which is induced by the change of electronic property and

Pure Appl. Chem.* **72, 1–331 (2000). An issue of reviews and research papers based on lectures presented at the 1st IUPAC Workshop on Advanced Materials (WAM1), Hong Kong, July 1999, on the theme of nanostructured systems.
†Corresponding author: E-mail address: zqtian@xmu.edu.cn

chemical environment of the substrate [14]. Accordingly, by using SERS effects and suitable adsorbate as probe molecule, one may be able to diagnose the special electronic properties of the metal nanoparticles in detail by analyzing the shift in band frequency and the intensity of the probe molecules.

The first stage of this approach is to prepare metal nanowire arrays and ensure that they can serve as the SERS substrate. To our knowledge, there is only one preliminary paper reported by Joo and Suh on SERS of Ag nanowire arrays about four years ago [10]. Ag nanowires were electrochemically deposited into the nanopores of anodic aluminum oxide (AAO) films followed by partial removal of the oxide layer to give rise to a strong SERS effect. The result obtained did not attract much attention, as the SERS intensity obtained was weaker than that from normally prepared Ag colloids. However, as has been known, the SERS effect is very complex and depends critically on many factors such as the size, shape, and dielectric constant of metals [15–17]. Therefore, it is essential to carry out the systematic study to extend the study on other metals, in particular some transition metals of both fundamental and practical importance. This is based on the recent progress made in our laboratory that many transition metals, such as Ni, Co, Fe, Pt, Pd, Rh, and Ru, exhibit weak SERS effect [18–23]. If the SERS effect of transition metals can be optimized by using nanowire arrays as the substrate, it may greatly renew interest in the SERS field for both the mechanism investigation and new applications. Accordingly, our present work has focused on a complementary study that is divided into two parts: (i) preparing the metal nanowire arrays as the substrate with high SERS activity, and (ii) developing the SERS to be a diagnostic tool to metal nanowires.

EXPERIMENTAL

The arrays were fabricated by means of the AAO templates. A large number of uniform nanoholes were arranged in two-dimensional array in the way of self-organizing by anodic oxidation. By controlling the applied voltage during the anodic oxidation, it is possible to prepare nanoholes with different diameter from 10 nm to 100 nm and the depth from 100 nm to 30 μm [24]. AC current was applied to deposit the metal into the pores. The parallel alignment of the cylindrical pores of aluminum oxide means that the nanowires deposited also aligned in one direction. Therefore, it enables us to deposit metal into the ordered nanoholes and get uniform metal nanowires with appropriate length through dissolving the aluminum oxide layer by dilute phosphoric acid for the maximum surface enhancement. Therefore, the quantitative calculation of the surface-enhancement factor (SEF) can be greatly simplified. The pore diameters were large enough (>10 nm) to form metal layers that have the properties of a metal. After the AAO film was chemically etched, layer by layer, to let the metal nanowires emerge gradually from the surface, SERS measurements were taken in sequence. Raman spectra were obtained using a confocal microprobe Raman system (LabRam I). The exciting wavelength was 632.8 nm from an internal He-Ne laser with a power of 12 mW on the sample surface. The detailed description on the Raman measurement has been given elsewhere [25]. The tapping mode AFM images were obtained on a scanning probe microscope (Nanoscope IIIa).

RESULTS AND DISCUSSION

Figure 1 shows AFM images of Cu nanowires after the aluminum oxide was removed partially. It can be seen that two-dimensional arrays of Cu nanowires were successfully fabricated by the AAO template synthesis method, and the wires were parallel to each other and normal to the surface (as shown in Fig. 1a). It is necessary to point out that the AFM tip is not sharp enough to go down to the bottom when the wire is longer than about 100 nm. Therefore, the AFM images are distorted to some extent due to the cone shape of the tip. On increasing the dissolution time, the length of Cu nanowires exposed on the surface became longer. Finally, the nanowires collapsed on the aluminum surface, and the length is more than 1 μm, as shown Fig. 1b. Then the more accurate data of the wire diameter was obtained by a

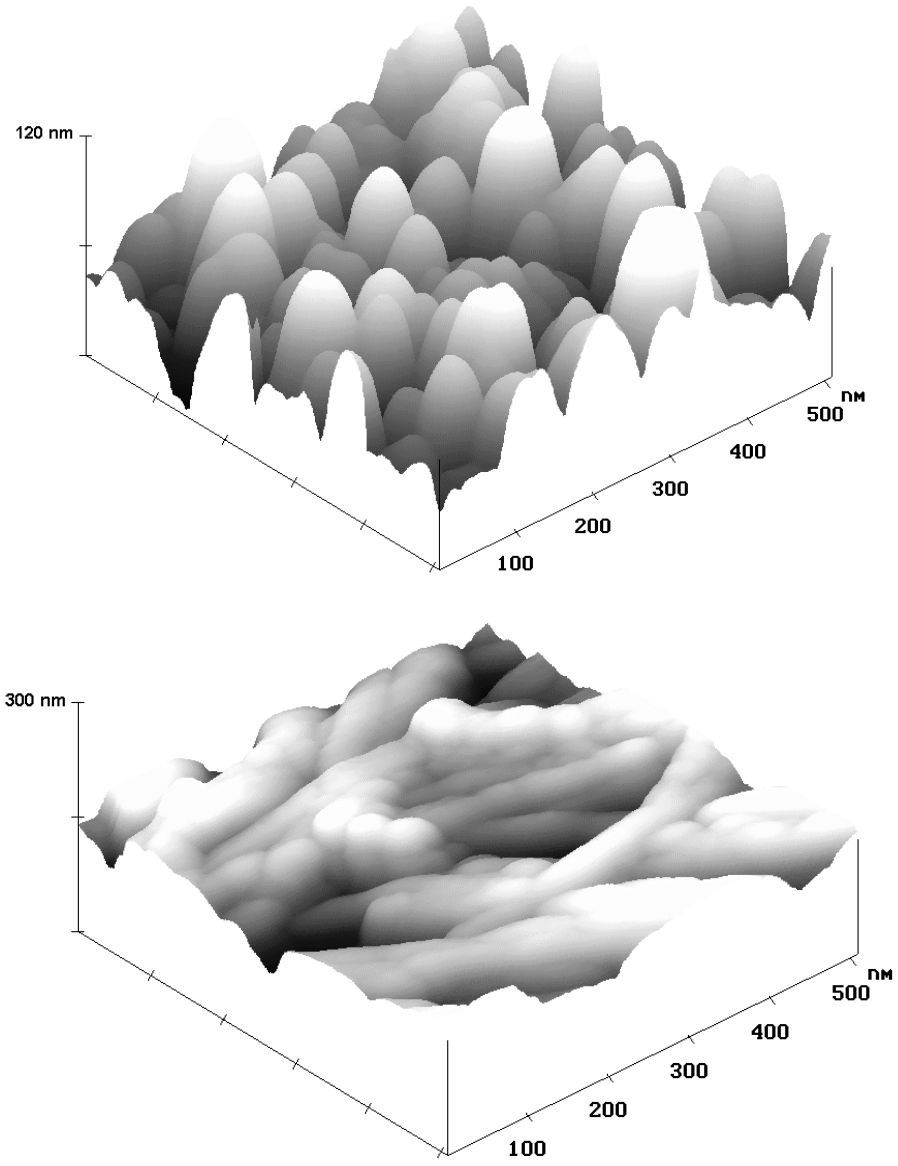

Fig. 1 AFM images of the Cu nanowires at the initial stage (a) and at the final stage (b) of the dissolution process to remove the AAO template.

transmission electron microscopy (JEM-200cx).

Fig. 2 presents the SERS spectra of pyridine adsorbed at different metal nanowires. The SERS signals observed are considerably stronger than that from the conventional roughened electrode surfaces. The SEF is calculated based on the method developed in our laboratory [26]. Five to six orders of the enhancement for noble metal of Au, Ag, and Cu and about three orders for Co and Ni nanowire arrays with their proper length have been obtained. This value is quite striking if we consider the fact that the SEF values are obtained from nanowires without applying any potential. It is worth noting that the SERS spectral features, including the frequency and relative band intensity, from the nanowires are

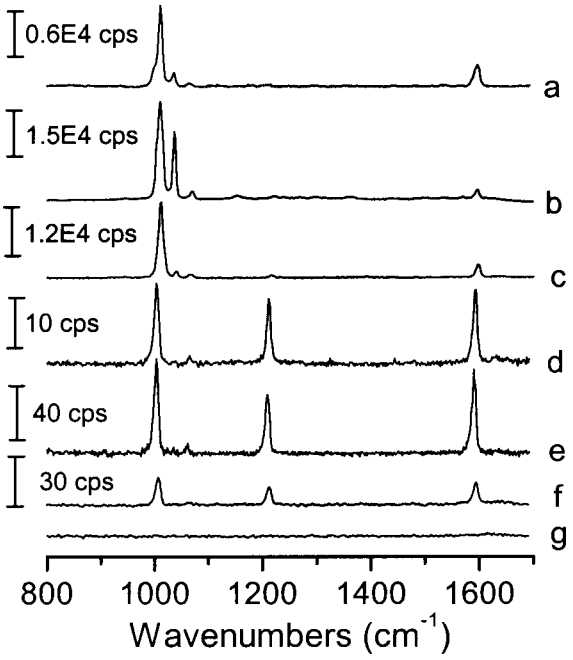

Fig. 2 The surface Raman spectra of pyridine adsorbed on different metal nanowires, Au (a), Ag (b), Cu (c), Co (d), Ni (e), and comparison with that obtained from an electrochemically roughened Ni electrode surface at the potential of –1.2 V (f) and around the open circuit potential (g). The solution was 0.01 M pyridine and 0.1 M KCl.

nearly identical to that of the normal bulk electrode at the open circuit potential. For the adsorbed pyridine at the noble and transition metal electrodes, its SERS intensity at the open circuit potential is normally three to ten times weaker than that at the optimized potential. For example, the three orders enhancement of the normal Ni electrode surface was obtained only from the optimized condition as the intensity reached the maximum at the potentials around –1.2 V, Fig. 2f. By contrast, the SERS intensity at the potentials of –0.6 V near the open circuit potential is remarkably weaker, Fig. 2g. If one takes the similar experimental condition (at the open circuit potential) into account, the SEF for the nanorod array is at least one order greater than that of the conventionally roughened electrodes of the same metal. It illustrates that metal nanowire arrays can serve as very good SERS active substrates, especially for transition metals.

It is well known that for the presence of large surface enhancement, the metal surfaces should be rough to some extent. The rough surface can be produced by various surface pretreatments, such as electrochemical oxidation-reduction cycles (ORC), chemical etching, vapor evaporation, or photochemical reduction [15]. However, the entire roughened surfaces are non-uniform, which will result in the different enhancement in the different area of the surface. To overcome this problem, numerous methods have been used to fabricate the ordered nanoparticles, such as lithography, metal colloids, and self-assemble layer technique, etc. [27–30]. However, no one can like the template synthesis method capable of well controlling both the diameter and aspect ratio of nanorods (nanowires) in a large area as regularly structured SERS substrates. Accordingly, it has been shown that the two-dimensional nanowire arrays are a kind of high active SERS substrates especially for transition metals of practical importance. Moreover, based on the above phenomenon, it is possible that the maximum enhancement can be achieved by carefully changing the diameter and length of the nanowires. This could be a key procedure to carry out the study on the complex SERS mechanism.

One of the most interesting spectral features is that the SERS intensity depends critically on the nanowire length emerged on the surface that was controlled by the etching time. For such a study, the time-dependent SERS measurement should be carried out. For acquiring SERS data within a shorter time such as 1 s, a Cu nanowire array exhibiting extremely high SERS activity was employed in this

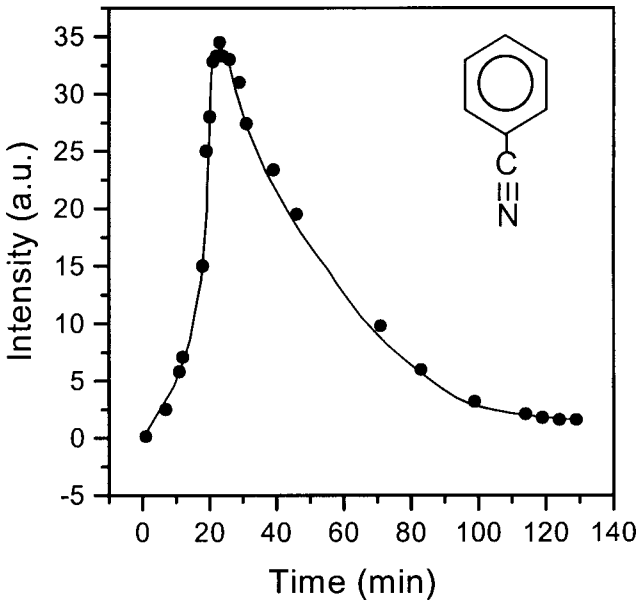

Fig. 3 The intensity-dissolution time profile of benzonitrile adsorbed at Cu nanowires (d ~30 nm). The solution was 0.02 M benzonitrile + 0.1 M $NaClO_4$.

study. During the chemical etching process, the band intensity of adsorbed benzonitrile at Cu nanowires became stronger and then reached a maximum that was about 30 times as strong as that at the initial stage and the end of the etching process. However, the intensity of SERS bands decreased with the etching time and almost remains unchanged after 140 min. (as shown in Fig. 3). Therefore, one can presume that the intensity–etching time dependence may be related to the complicated SERS mechanisms rather than the change of coverage. The theoretical and experimental studies of the enhanced mechanisms indicate that SERS effect is mainly contributed by the EM enhancement in many cases [15,17]. A major contribution to the electromagnetic enhancement is due to surface plasmon (SP) resonance for the noble metals. However, SP is not the only source of enhanced local electromagnetic fields. Another type of enhanced electromagnetic field lies near high-curvature points on the rough surface. The classic theoretical calculation of enhancement for a metal prolate spheroid mode revealed that the maximum enhancement could be obtained at the tip of the spheroid and increased with the aspect ratio [31,32]. This effect is called the lightning-rod effect, in which the electric field is largest near the sharpest surface of the needle-like rod based on the calculation results. In the present case, the cylindroid nanowires could be considered as separated prolate spheroids standing at the surface. In the initial stage of the dissolution of the alumina template, the length of the emerged metal was rather short. With the increase of the length of Cu nanowires standing up at the surface, the aspect ratio becomes larger. One may assume that the electric field at the top of the ellipsoid reached its maximum under the favorable length of metal nanowires. Therefore, the intensity of the adsorbed molecule changed with the etching time and passed a maximum, since the aspect ratio of the wire deviated more and more from the favorable value. At the end of the dissolution process, it is impossible for the nanowires to support themselves on the surface when the nanowires became longer and longer. As a result, they collapsed at the alumina surface, and the surface structure changed totally. Therefore, the prolate spheroid mode was not suitable for this kind of surface, at which the metal nanowires lay down randomly. At last, the intensity of Raman signal decreased substantially and reached a constant value. Accordingly, the lightning-rod effect may play an important role for the enhancement in addition to the SP resonance enhancement, and this effect needs to be considered for a complete understanding of SERS mechanisms.

It is of special interest to take the advantages of SERS to characterize the novel properties of the metal nanowires by selecting a suitable probe molecule that is very sensitive to any change of the surface structure. In our case, the SCN^- ion was used as the surface probe because the SCN^- band frequency and shape are very sensitive to the surface property, including electrostatic environment [33,34]. Fig. 4 represents the SERS spectra of SCN^- adsorbed at Cu nanowires with different diameter; the insertion shows the frequency-diameter plot. It can be seen that the diameter of the nanowires influences the frequency of the adsorbed SCN^- distinctly; i.e., the frequency blue-shifts in about 20 cm^{-1} with the increase of the diameter from 15 to 50 nm. When the diameter was larger than about 50 nm, the frequency of C ≡ N stretching vibration (ν_{CN}) of the adsorbed SCN^- approached a constant value, and was close to that from the roughened bulk Cu electrodes at the open circuit potential. This may infer that the property of large-diameter nanowires is similar to that of the bulk metals. Our previous studies of SCN^- adsorbed on the normal Cu electrode showed that the ν_{CN} decreases, with the electrode potential moving negatively. This is mainly due to the greater tendency to give electrons at the more negative potential, leading the down-shift of the ν_{CN} [33,34]. In our present investigation, all measurements were carried out at the open circuit potential as the nanowires are within the AAO film as electronic insulator. Therefore, the frequency–diameter dependence may result from other factors.

Fermi level is well known to be one of the most important parameters characterizing a metal since its value determines the gross electronic properties that could consequently influence the relevant vibrational frequency of the adsorbate. To move the applied electrode potential negatively would cause the up-shift of the Fermi level and the greater tendency to give electrons from the electrode to the adsorbate. The Fermi level of a metal nanorod could be estimated in a simple way by considering free electrons confined to a cylinder box of length *l* and radius *r*. The energy level in atomic units is given by:

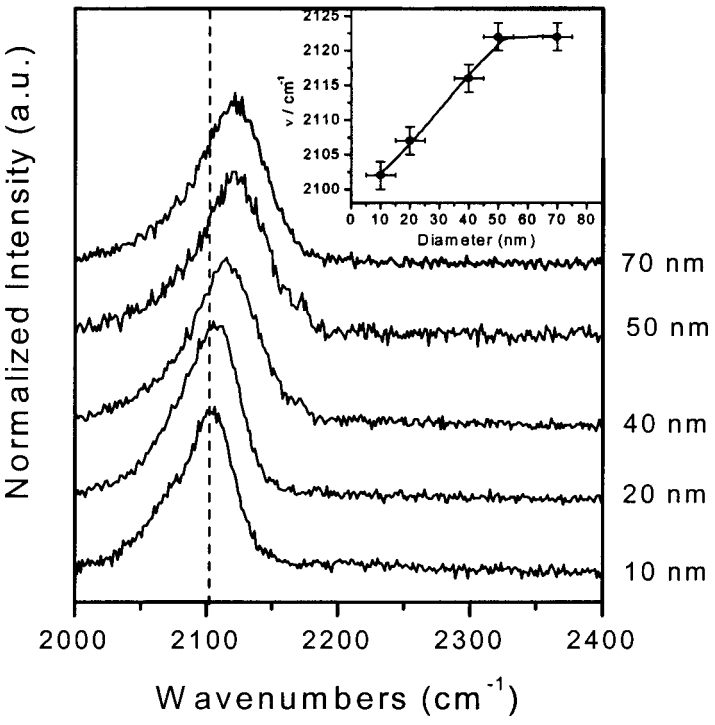

Fig. 4 In situ SERS spectra of SCN^- adsorbed at the Cu nanowires with different diameters. The solution was 0.01 M NaSCN and 4% H_3PO_4.

$$E = \frac{n^2\pi^2}{l^2} + \frac{C_m^2}{r^2} \qquad n = 1,2,3,...; m = 0,\pm 1,\pm 2,....$$

where C_m is a parameter determined by the Bessel function. This equation indicates, at least qualitatively, that the Fermi level of the nanorod would shift up as the diameter decreases. The more detailed discussion on this aspect will be given elsewhere [35].

In summary, the developments of SERS and the metal nanowire materials are obviously mutually beneficial and complementary in their studies. The ordered metal nanowires, especially the transition metal nanowires, with suitable dimension can serve as high SERS active substrates, which are better than the normal roughened surfaces. Taking the template-synthesized strategy, one will be able to get a deeper insight into the complicated SERS mechanism(s) by fabricating ordered nanostructuring surfaces with regular shape, size, and length of nanorods (nanowires) for the systematic investigation. On the other hand, by taking the probe molecule strategy, the SERS could be a diagnostic tool to probe the electronic properties and even optical properties if surface-enhanced resonance Raman scattering (SERRS) is applied. Moreover, SERS could be developed as an *in situ* tool in monitoring the etching process of metal nanowires with various length and diameter.

ACKNOWLEDGMENTS

The authors gratefully acknowledge the financial support from the Natural Science Foundation of China and the Ministry of Education of China.

REFERENCES

1. C. R. Martin. *Science* **266**, 1961 (1994).
2. S. Link, Z. L. Wang, M. A. El-Sayed. *J. Phys. Chem. B* **103**, 3529 (1999).
3. J. C. Hulteen and C. R. Martin. Chapter 10 in *Nanoparticles and Nanostructured Films* (J. H. Fendler, ed.) Wiley-VCH, Weinheim (1998).
4. B. B. Li, D. P. Yu, S. L. Zhang. *Phys. Rev. B* **59**, 1645 (1999).
5. C. K. Preston, M. Moskovits. *J. Phys. Chem.* **92**, 2957 (1988).
6. C. A. Foss, J. Gabor, L. Hornyak, J. A. Stockert, C. R. Martin. *J. Phys. Chem.* **98**, 2963 (1994).
7. C. K. Preston and M. Moskovits. *J. Phys. Chem.* **97**, 8495 (1993).
8. N. A. F. Al-Rawashdeh, M. L. Sandrock, C. J. Seudling, C. A. Foss. *J. Phys. Chem. B* **102**, 361 (1998).
9. D. Routkevitch, T. L. Haslett, L. Ryan, T. Bigioni, C. Douketis, M. Moskovits. *Chem. Phys.* **210**, 343 (1996).
10. Y. Joo and J. S. Suh. *Bull. Korean Chem. Soc.* **16**, 808 (1995).
11. J. S. Suh and J. S. Lee. *Chem. Phys. Lett.* **281**, 384 (1997).
12. P. M. Aiayan. *Chem. Rev.* **99**, 1787 (1999).
13. D. A. Weitz, T. J. Gramila, A. Z. Genack, J. I. Gersten. *Phys. Rev. Lett.* **45**, 355 (1980).
14. V. M. Browne, S. G. Fox, P. Hollins. *Catal. Today* **9**, 1 (1991).
15. M. Moskovits. *Rev. Mod. Phys.* **57**, 783 (1985).
16. A. Otto, I. Mrozek, H. Grabhorn, W. Akemann. *J. Phys. Condens. Matter* **4**, 1143 (1992).
17. A. Campion and P. Kambhampati. *Chem. Soc. Rev.* **27**, 241 (1998)
18. B. Ren, Q. J. Huang, W. B. Cai, B. W. Mao, F. M. Liu and Z. Q. Tian. *J. Electroanal. Chem.* **415**, 175 (1996).

19. Z. Q. Tian, B. Ren, B. W. Mao. *J. Phys. Chem. B* **101**, 1338 (1997).
20. J. S. Gao and Z. Q. Tian. *Spectrochim. Acta A* **53**, 1595 (1997).
21. Q. J. Huang, J. L. Yao, B. W. Mao, R. A. Gu, Z. Q. Tian. *Chem. Phys. Lett.* **271**, 101 (1997).
22. B. Ren, X. Xu, X. Q. Li, W. B. Cai, Z. Q. Tian. *Surf. Sci.* **427–428**, 157 (1999).
23. Z. Q. Tian, J. S. Gao, X. Q. Li, B. Ren, Q. J. Huang, W. B. Cai, F. M. Liu, B. W. Mao. *J. Raman Spectrosc.* **29**, 703 (1998).
24. S. Shingubara, O. Okino, Y. Sayama, H. Sakaue, T. Tanahagi. *Jpn. J. Appl. Phys.* **36**, 7791 (1997).
25. B. Ren, Z. Q. Tian. submitted to *Anal. Chem.*
26. W. B. Cai, B. Ren, X. Q. Li, C. X. She, F. M. Liu, X. W. Cai, Z. Q. Tian. *Surf. Sci.* **406**, 9 (1998).
27. P. F. Liao, J. G. Bergman, D. S. Chemla, A. Wokaun, J. Melngailis, A. M. Hawryluk, N. P. Economou. *Chem. Phys. Lett.* **82**, 355 (1981).
28. K. Kneipp, Y. Wang, H. Kneipp, L. T. Perelman, I. Itzkan, R. R. Dasari, M. S. Feld. *Phys. Rev. Lett.* **78**, 1667 (1997).
29. S. Nie and S. R. Emory. *Science* **275**, 1102 (1997).
30. R. G. Freeman, K. C. Grabar, K. J. Allison, R. M. Bright, J. A. Davis, A. P. Guthrie, M. B. Hommer, M. A. Jackson, P. C. Smith, D. G. Walter, M. J. Natan. *Science* **267**, 5204 (1995).
31. J. Gersten and A. Nitzan, *J. Chem. Phys.* **73**, 3023 (1980).
32. J. I. Gersten. *J. Chem. Phys.* **73**, 5799 (1980).
33. Z. Q. Tian, W. H. Li, Z. H. Qiao, W. F. Lin, Z. W. Tian. *Russian J. Electrochem.* **31**, 1014 (1995).
34. M. J. Weaver, F. Barz, J. G. Gordon, M. R. Philoptt. *Surf. Sci.* **125**, 409 (1983).
35. X. Xu, D. Y. Wu, J. L. Yao, Z. Q. Tian. to be submitted.